Precision QCD calculation for top-pair production at lepton collider in the continuum

Hua Xing Zhu
Massachusetts Institute of Technology

Workshop on Top physics at the LC 2016
July 7th, KEK

Perspective precision on top EW coupling from ILC

Amjad et al., EPCJ75(2015),10, 512

$$\Gamma_{\mu}^{t\bar{t}X}(k^2, q, \bar{q}) = ie\left\{\gamma_\mu\left(F_{1V}^X(k^2) + \gamma_5 F_{1A}^X(k^2)\right) - \frac{\sigma_{\mu\nu}}{2m_t}(q+\bar{q})^\nu\left(iF_{2V}^X(k^2) + \gamma_5 F_{2A}^X(k^2)\right)\right\}$$

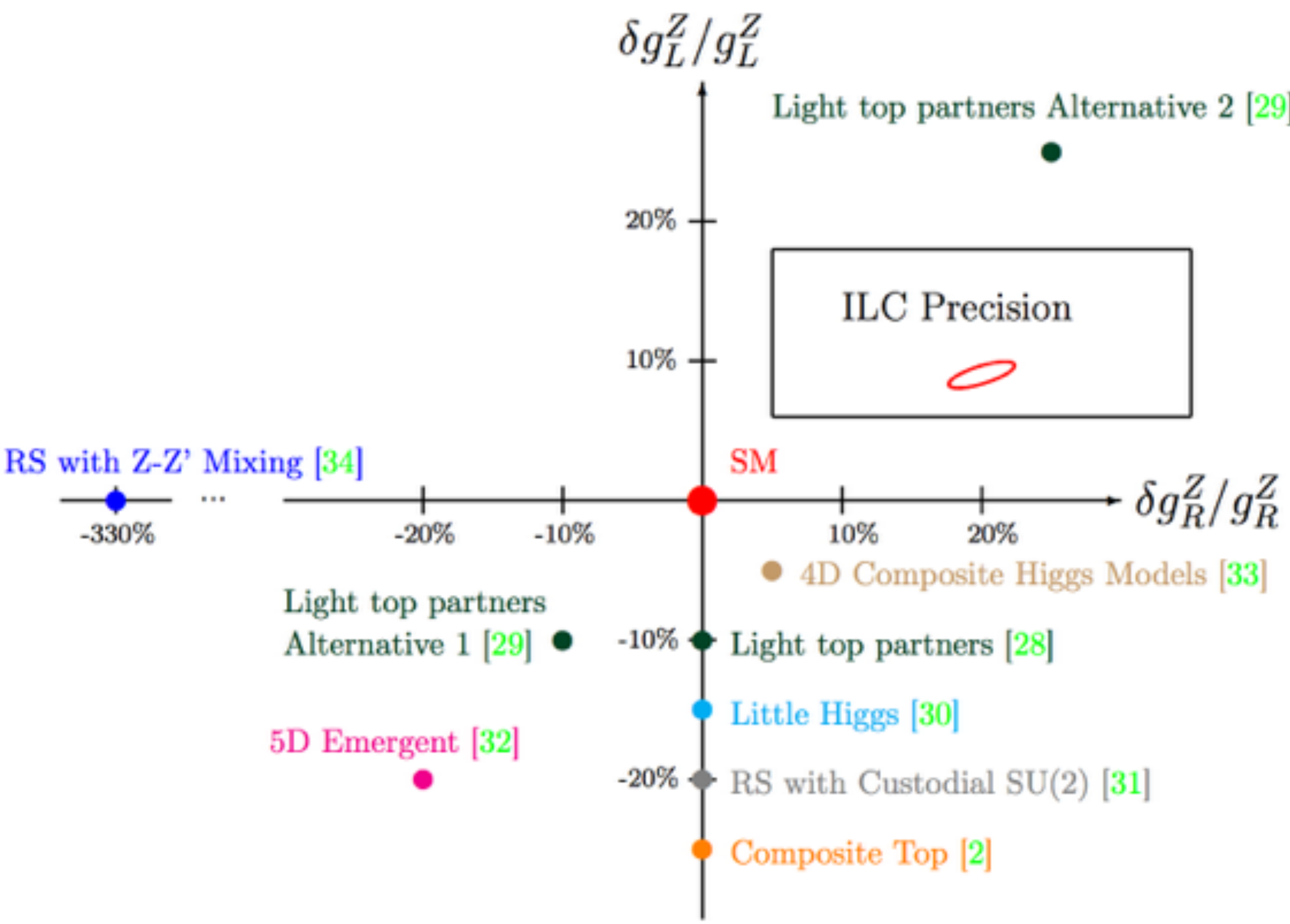

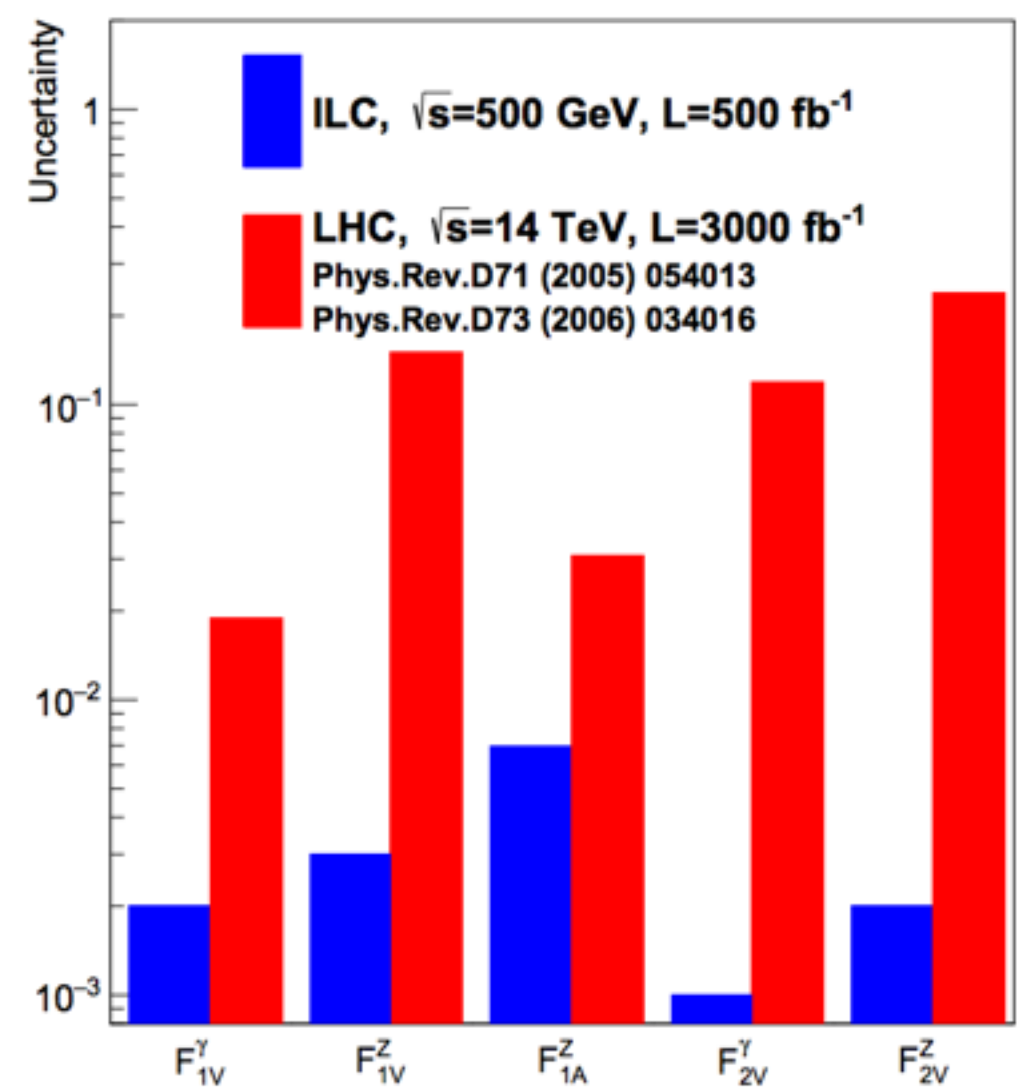

Theoretical effort on precision

- QCD N3LO tT production at threshold [Beneke, et al., PRL115, 192001 (2015)]
- QCD N3LO inclusive cross section in high energy expansion up to $(m^2/s)^6$ [Chetyrkin et al., NPB503, 339 (1997)]
- Boosted top jet production at NLL [Fleming et al., PRD77(2008) 114003]
- One-loop EW corrections [Fleischer et al., EPJC31 (2003) 37]
- QCD NLO event generator including parton shower in WHIZARD
- One-loop EW corrections in GRACE
- …

This talk: tT production in the continuum at QCD NNLO

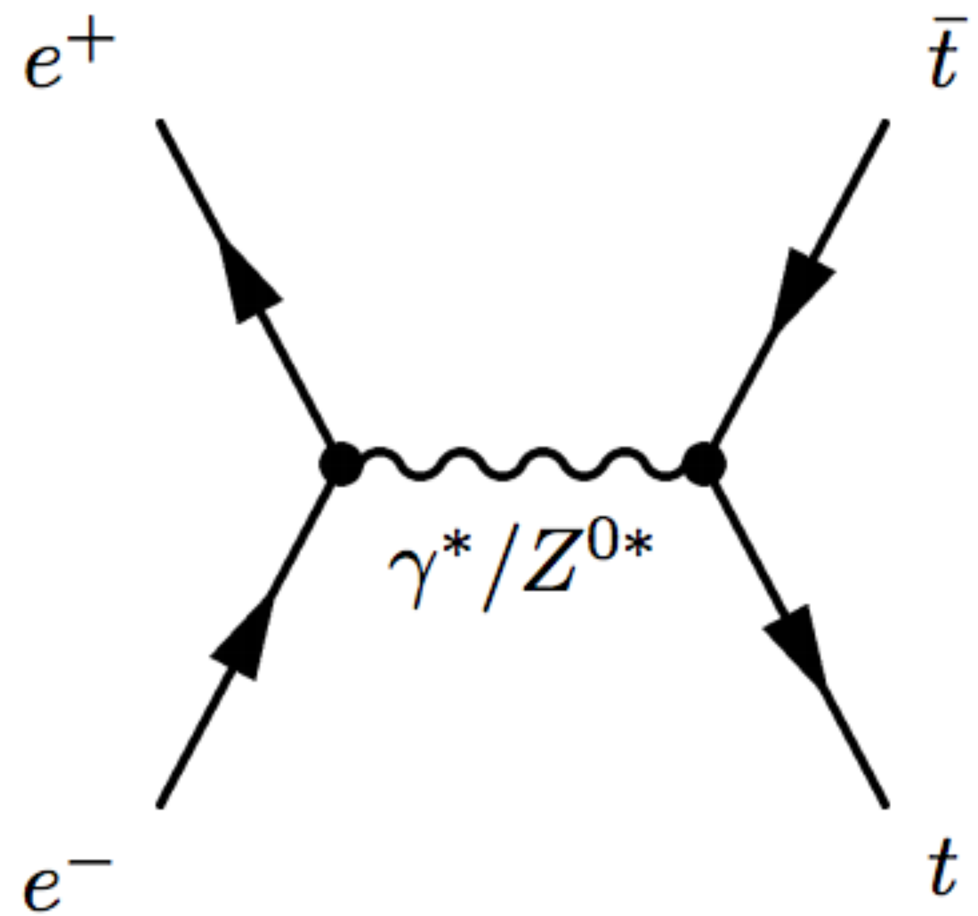

$$\sqrt{S} = 380, 500, 750, 1000? \text{ GeV}$$

Fully differential in top quark kinematics

tT production in the continuum at QCD NNLO

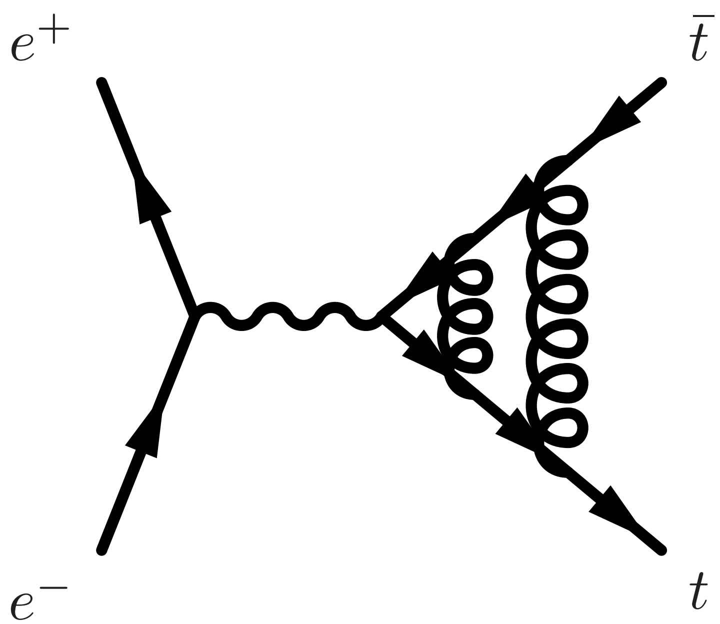

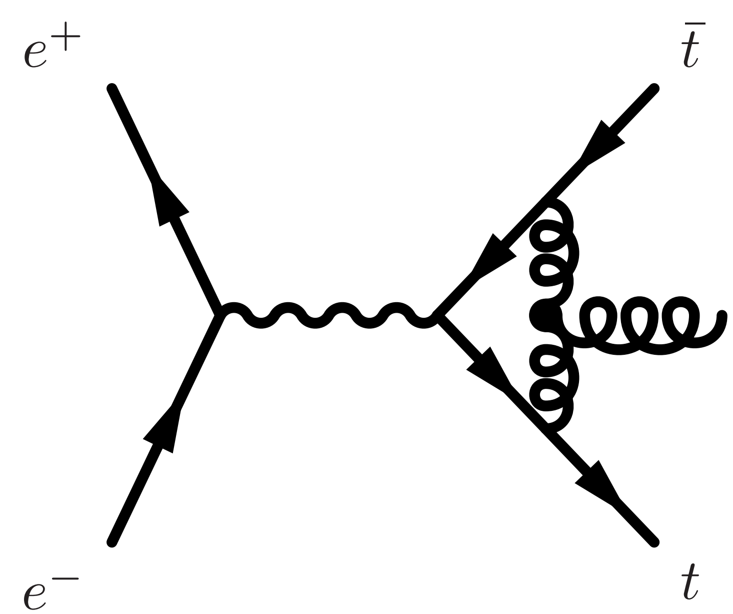

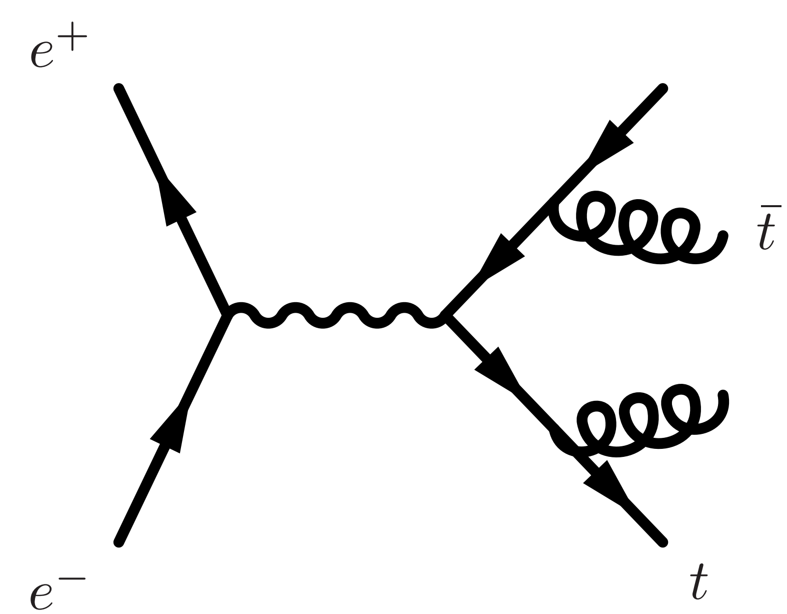

double virtual

two-loop heavy quark form factor

real-virtual **double real**

NLO QCD corrections to tT + jet production

Two-loop heavy quark form factor

$$\Gamma_\mu^{t\bar{t}X}(k^2,q,\bar{q}) = ie\left\{\gamma_\mu\left(F_{1V}^X(k^2)+\gamma_5 F_{1A}^X(k^2)\right) - \frac{\sigma_{\mu\nu}}{2m_t}(q+\bar{q})^\nu\left(iF_{2V}^X(k^2)+\gamma_5 F_{2A}^X(k^2)\right)\right\}$$

- **The calculation of heavy quark form factor has been a subject of strong theoretical interest for a long time**
- **Two-loop contribution with closed fermion loops [Hoang et al., PLB338 (1994) 330]**
- **Full two-loop results available 10 years later [Bernreuther et al., NPB706, 245(2005); NPB712, 229(2005)]**
- **Application of many cutting-edge techniques at the time: integration-by-parts identities, Lorentz invariance, Laporta algorithm, method of differential equation**
- **Results written with 50 pages of harmonic polylogarithms.**

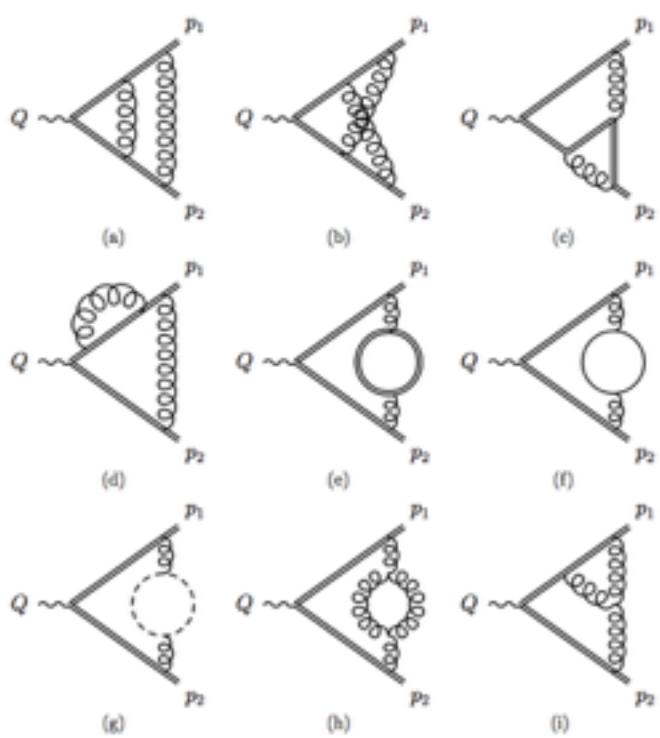

heavy quark pair + jet at NLO

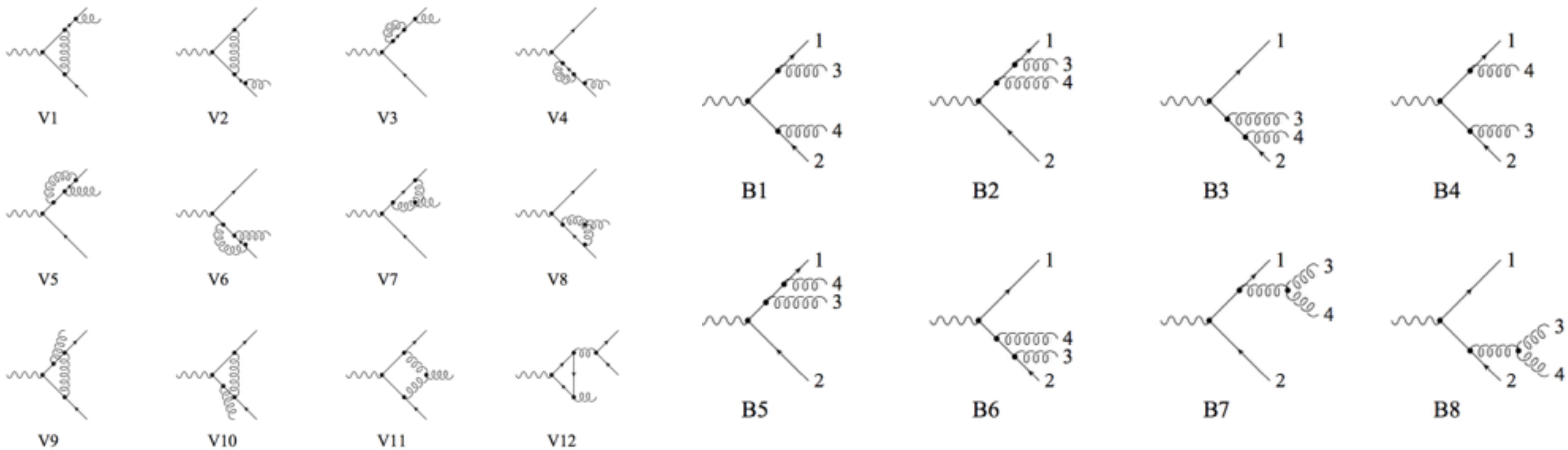

- **NLO calculation available for about twenty years [Brandenburg, Uwer, NPB515(1998)279; Nason, Oleari, NPB521(1998)237; Rodrigo, Bilenky, Santamaria, NPB554(1999)257]**
- **These used to be difficult calculation. The remarkable progress in calculation technique for one-loop amplitude, and NLO subtraction of infrared/collinear singularity make such calculation "almost" trivial nowadays. For example can be automated using tools like Gosam.**

tT+X at QCD NNLO

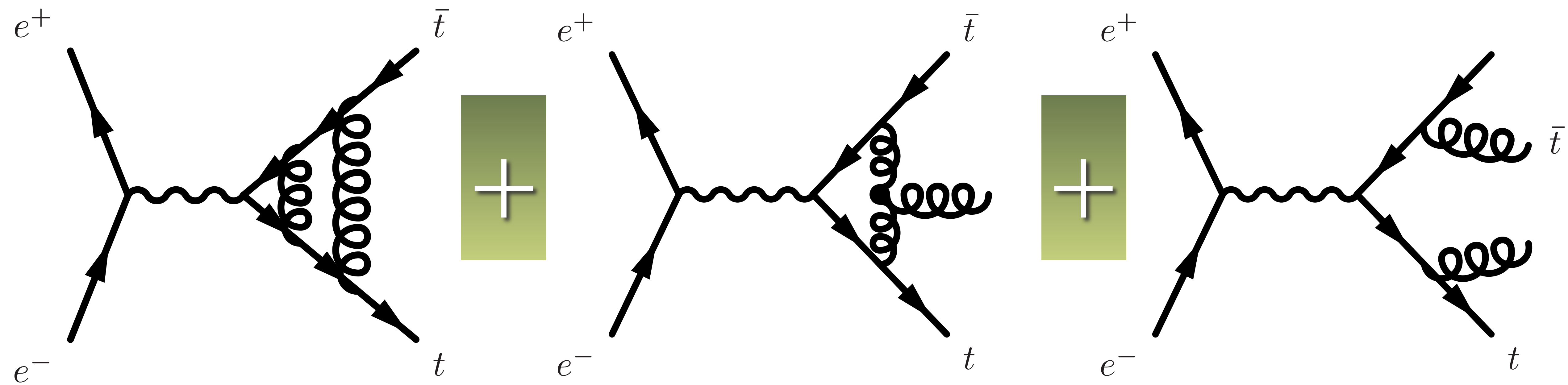

double virtual

$$\frac{A_1}{\epsilon_{\mathrm{IR}}^2} + \frac{B_1}{\epsilon_{\mathrm{IR}}}$$

real-virtual

$$\frac{A_2}{\epsilon_{\mathrm{IR}}^2} + \frac{B_2}{\epsilon_{\mathrm{IR}}}$$

double real

$$\frac{A_3}{\epsilon_{\mathrm{IR}}^2} + \frac{B_3}{\epsilon_{\mathrm{IR}}}$$

For IR-safe cross section

$$\sum_i A_i = 0 \qquad \sum_i B_i = 0$$

tT+X at QCD NNLO

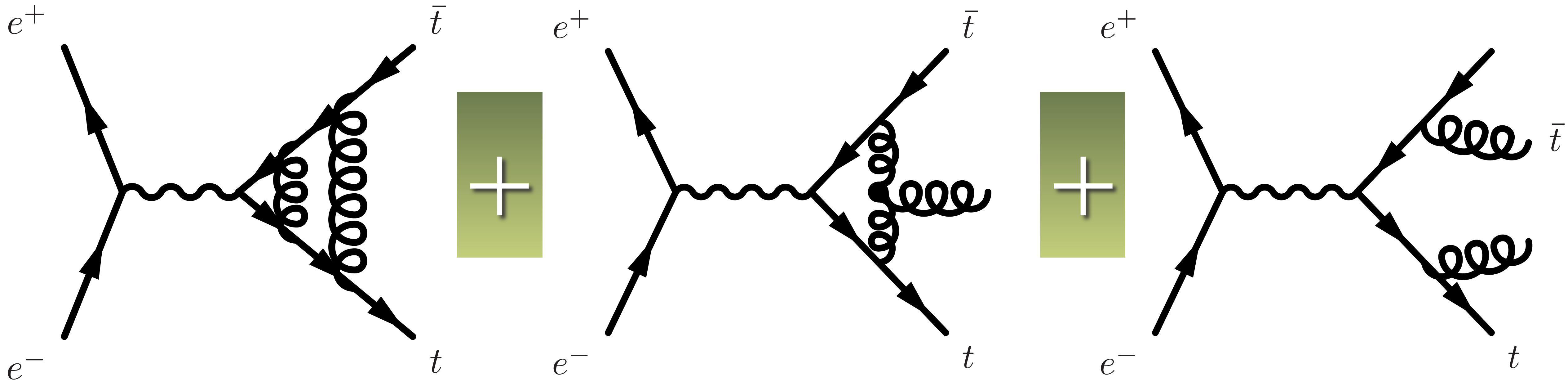

double virtual **real-virtual** **double real**

- **The infrared divergences origin from the real or virtual gluons become soft**
- **In the double virtual corrections, the IR poles are manifest, while in the real-virtual and double real they come from phase space integration**
- **The most successful method to deal with these poles at NLO is the subtraction, but at NNLO becomes too tedious**
- **Instead we generalize the more phase space slicing method to NNLO to overcome this problem**

Phase space slicing using radiation energy

von Manteuffel, Schabinger, H.X.Z, PRD92(2015)no.4,045034; J. Gao, H.X.Z, PRD90.114022; J. Gao, H.X.Z, PRL113(2014)262001

E_x: energy of QCD radiations from heavy quark pair

resolved part $E_X > Q\delta_E$

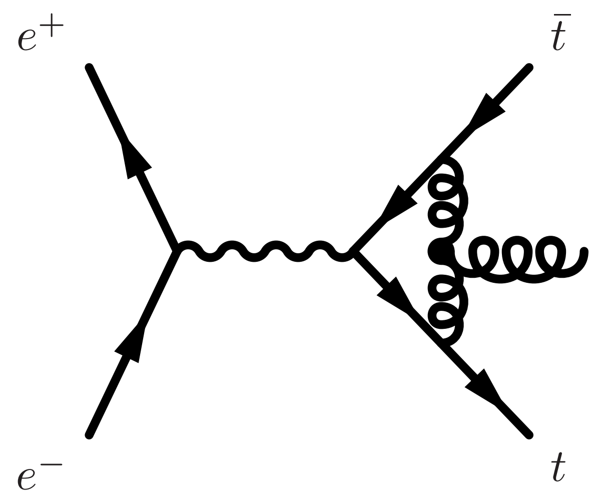

$\widetilde{C}_2 \ln^2 \delta_E + \widetilde{D}_2 \ln \delta_E$

+

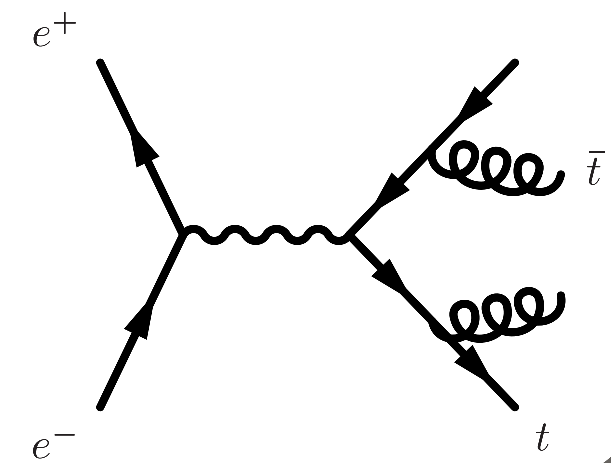

$\widetilde{C}_3 \ln^2 \delta_E + \widetilde{D}_3 \ln \delta_E$

unresolved part $E_X < Q\delta_E$

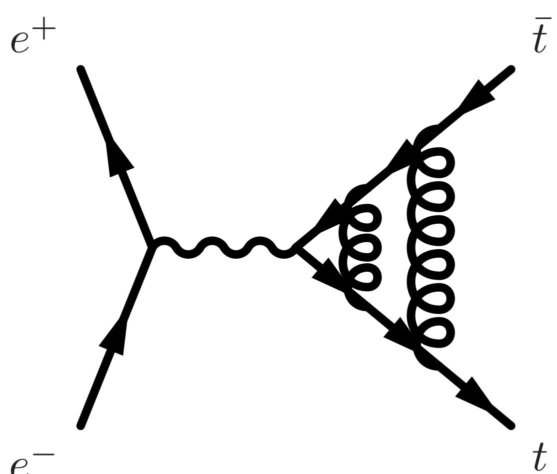

$$\frac{A_1}{\epsilon_{\mathrm{IR}}^2} + \frac{B_1}{\epsilon_{\mathrm{IR}}}$$

+

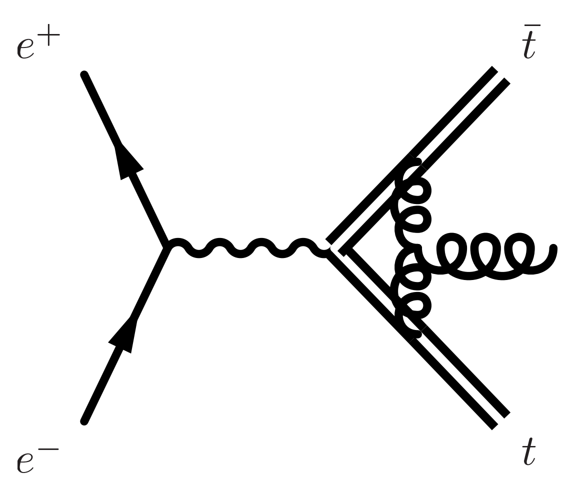

$$\frac{A_2}{\epsilon_{\mathrm{IR}}^2} + \frac{B_2}{\epsilon_{\mathrm{IR}}} + \widetilde{A}_2 \ln^2 \delta_E + \widetilde{B}_2 \ln \delta_E$$

+

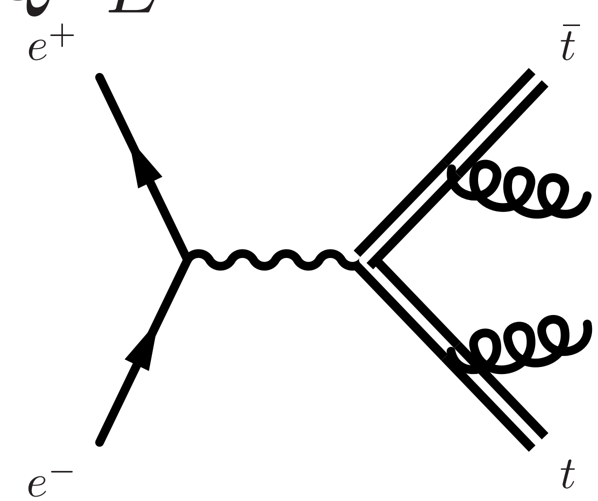

$$\frac{A_3}{\epsilon_{\mathrm{IR}}^2} + \frac{B_3}{\epsilon_{\mathrm{IR}}} + \widetilde{A}_3 \ln^2 \delta_E + \widetilde{B}_3 \ln \delta_E$$

Classical color source moving at velocity v

Analytic calculation of the unresolved part

von Manteuffel, Schabinger, H.X.Z, PRD92(2015)no.4,045034

- The difficult phase space integral reduces to calculation of matrix element of time-like Wilson loop
- Can be treated analytically
- Results written in about two pages of harmonic polylogarithms

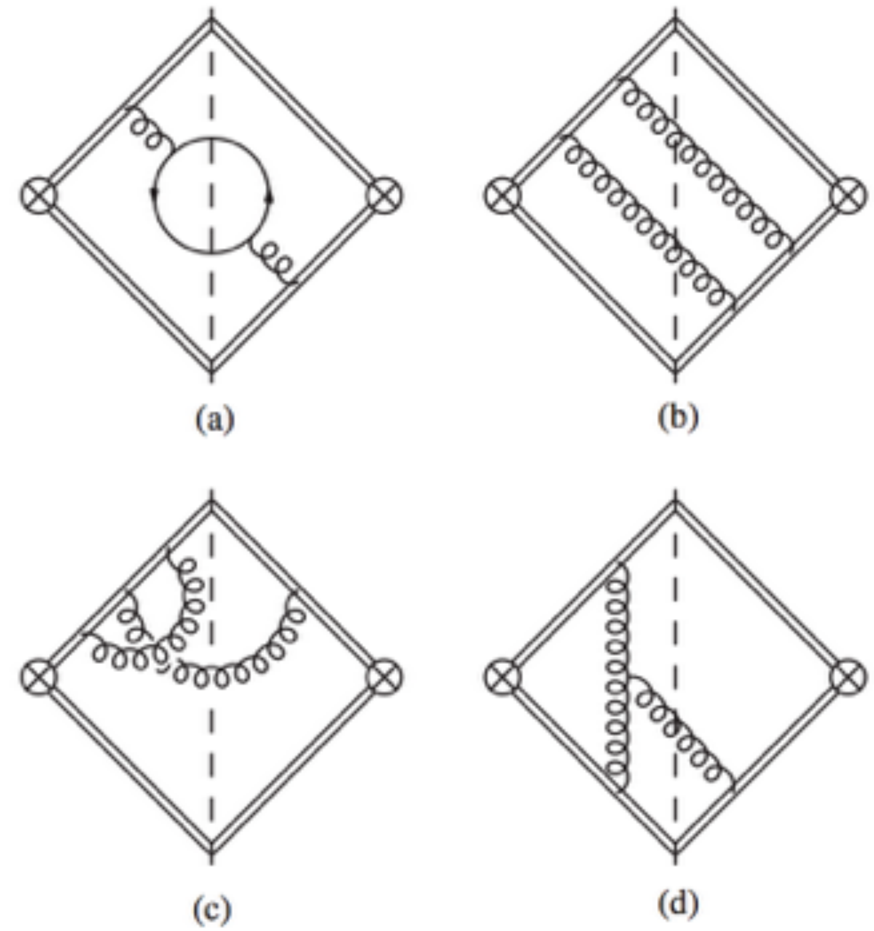

$$
\begin{aligned}
c_2(x) = {} & C_F^2\Big[2\frac{(1+x^2)^2}{(1-x^2)^2}\Big(G^4(0;x) - 8G(1;x)G^3(0;x) + 8\Big(2G^2(1;x) + G(0,1;x) + \frac{\pi^2}{6}\Big)G^2(0;x) \\
& -32\Big(G(0,1;x) + \frac{\pi^2}{6}\Big)G(1;x)G(0;x) + 16G^2(0,1;x) + \frac{16\pi^2}{3}G(0,1;x) + \frac{4\pi^4}{9}\Big) \\
& +8\frac{(1+x^2)}{(1-x)^2}\Big(G^2(0;x) - 4G(1;x)G(0;x) + 4G(0,1;x) + \frac{2\pi^2}{3}\Big)G(0;x) + 8\frac{(1+x)^2}{(1-x)^2}G^2(0;x)\Big] \\
& + C_F n_f T_F\Big[-\frac{224}{27} + \frac{16(1-3x+x^2)}{9(1-x^2)}\Big((G(0;x) - 4G(1;x))G(0;x) + 4G(0,1;x) + \frac{2\pi^2}{3}\Big) \\
& + \frac{8(1+x^2)}{3(1-x^2)}\Big(-\frac{1}{3}G^3(0;x) + 2G(1;x)G^2(0;x) - 4\Big(G^2(1;x) + \frac{\pi^2}{6}\Big)G(0;x) + \frac{4\pi^2}{3}G(1;x) \\
& +8G(1;x)G(0,1;x) - 4G(0,0,1;x) - 8G(0,1,1;x) + 4\zeta(3)\Big) + \frac{16(1+30x+x^2)}{27(1-x^2)}G(0;x)\Big] \\
& + C_A C_F\Big[-\frac{2(11x^4 - 84x^3 + 24x^2 + 12x - 11)}{9(1-x^2)^2}G^3(0;x) + \frac{4(55x^2 - 294x + 55)}{27(1-x^2)}G(0;x) \\
& + \frac{4(17x^3 - 32x^2 + 68x - 17)}{9(1-x^2)(1-x)}G^2(0;x) + \frac{8\pi^2(5x^4 + 27x^3 + 6x^2 + 3x + 7)}{9(1-x^2)^2}G(0;x) \\
& -4\zeta(3)\frac{(1+x^2)(9+x^2)}{(1-x^2)^2}G(0;x) + \frac{4\pi^2(11x^2 + 66x - 25)}{27(1-x^2)} + \frac{\pi^4(1+x^2)(77+221x^2)}{90(1-x^2)^2} \\
& + \frac{16(26x^2 - 33x + 26)}{9(1-x^2)}(G(0;x)G(1;x) - G(0,1;x)) + \frac{8\pi^2(1+x^2)(3+7x^2)}{3(1-x^2)^2}(G(0,1;x) \\
& -G(0;x)G(1;x)) + 8\frac{3x^3 - 7x^2 - 5x + 1}{(1-x^2)(1-x)}(G(-1;x)G^2(0;x) - 2G(0,-1;x)G(0;x) \\
& +2G(0,0,-1;x)) + 16\frac{x^3 - x^2 + 3x + 1}{(1-x^2)(1+x)}(2G(0,0,-1;x) - G(0;x)G(0,-1;x)) \\
& + \frac{8(13x^4 - 72x^2 + 11)}{3(1-x^2)^2}(2G(0,0,1;x) - G(0;x)G(0,1;x)) - 8\frac{(1+x^2)(3x^2-1)}{(1-x^2)^2} \\
& \times(6G(0,0,0,-1;x) + G(0,-1;x)G^2(0;x) - 4G(0,0,-1;x)G(0;x)) \\
& + \frac{1+x^2}{1-x^2}\Big(\frac{8}{3}G(-1;x)G^3(0;x) + \Big(\frac{4}{3}G(1;x) - 8G(0,-1;x)\Big)G^3(0;x) + (24G^2(-1;x) \\
& -16G(1;x)G(-1;x) - \frac{16\pi^2}{3}G(-1;x) - 16G(-1;x) + \frac{16}{3}G^2(1;x) - \frac{8}{3}G(0,1;x)\Big)G(0;x) \\
& - \frac{4\pi^2}{3}G(-1;x) - \frac{100\pi^2}{9}G(1;x) - 48G(-1;x)G(0,-1;x) + 16G(1;x)G(0,-1;x)
\end{aligned}
$$

$$
\begin{aligned}
& + \frac{16\pi^2}{3}G(0,-1;x) + 16G(0,-1;x) + 16G(-1;x)G(0,1;x) - \frac{32}{3}G(1;x)G(0,1;x) \\
& +48G(0,-1,-1;x) - 16G(0,-1,1;x) + \frac{8}{3}G(0,0,1;x) - 16G(0,1,-1;x) + \frac{32}{3}G(0,1,1;x) \\
& + 32G(0,0,0,-1;x)) + \frac{(1+x^2)(1+3x^2)}{(1-x^2)^2}\Big(\frac{8}{3}G(1;x)G^3(0;x) + 16G(0,0,1;x)G(0;x) \\
& +\Big(\frac{2\pi^2}{3} - 8G(0,1;x)\Big)G^2(0;x) - 16G(0,0,0,1;x)\Big) + \frac{x^2(1+x^2)}{(1-x^2)^2}\Big(-\frac{4}{3}G^4(0;x) \\
& +96G(0,0,1;x)G(0;x) - 288G(0,0,0,1;x)\Big) + \frac{(1+x^2)^2}{(1-x^2)^2}(16G(0,1;x)G^2(0;x) \\
& +(16G(0,1,-1;x) - 64G(0,0,1;x) - 32G(1;x)G(0,1;x) + 48G(0,-1,-1;x) \\
& -32G(1;x)G(0,-1;x) + 16G(0,-1,1;x) + 16G(0,1,1;x))G(0;x) - 24G^2(0,-1;x) \\
& +8G^2(0,1;x) - \frac{4\pi^2}{3}G(0,-1;x) - \frac{4\pi^2}{3}G(0,1;x) + 16G(0,-1;x)G(0,1;x) \\
& +64G(1;x)G(0,0,-1;x) + 64G(1;x)G(0,0,1;x) - 64G(0,0,-1,1;x) + 96G(0,0,0,1;x) \\
& -64G(0,0,1,-1;x) + 16G(1;x)\zeta(3) - 64G(0,0,1,1;x) - 32G(0,1,0,-1;x)) \\
& + \frac{4\zeta(3)(13x^4 - 12x^2 - 49)}{3(1-x^2)^2} + \frac{592}{27}\Big].
\end{aligned}
$$

Validating the calculation: cancellation of slicing parameter δ_E

J. Gao, H.X.Z, PRD90.114022

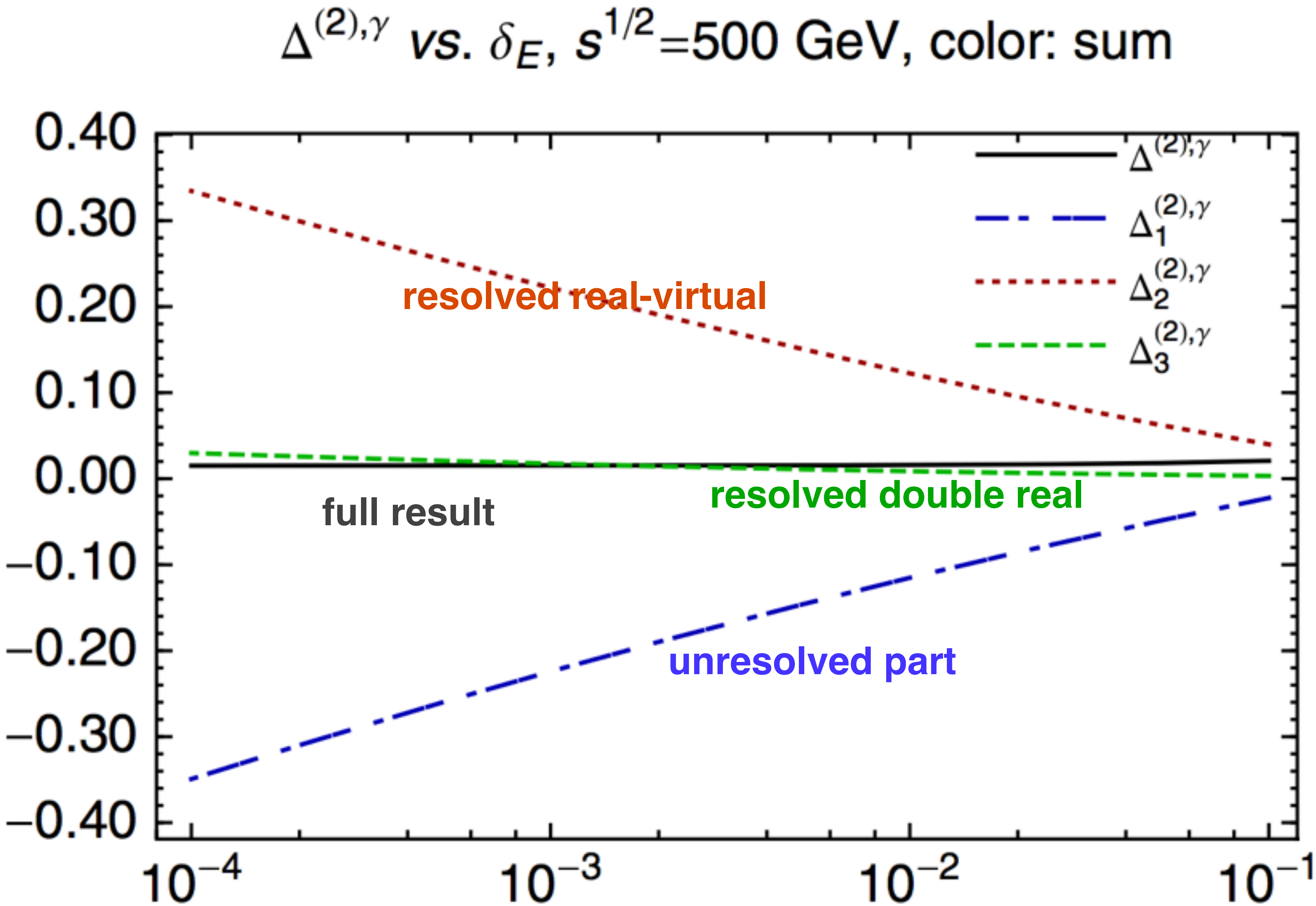

$$\sigma_{\mathrm{NNLO},\gamma} = \sigma_{\mathrm{LO},\gamma}(1 + \Delta^{(1),\gamma} + \Delta^{(2),\gamma})$$

Validating the calculation: cancellation of slicing parameter δ_E

J. Gao, H.X.Z, PRD90.114022

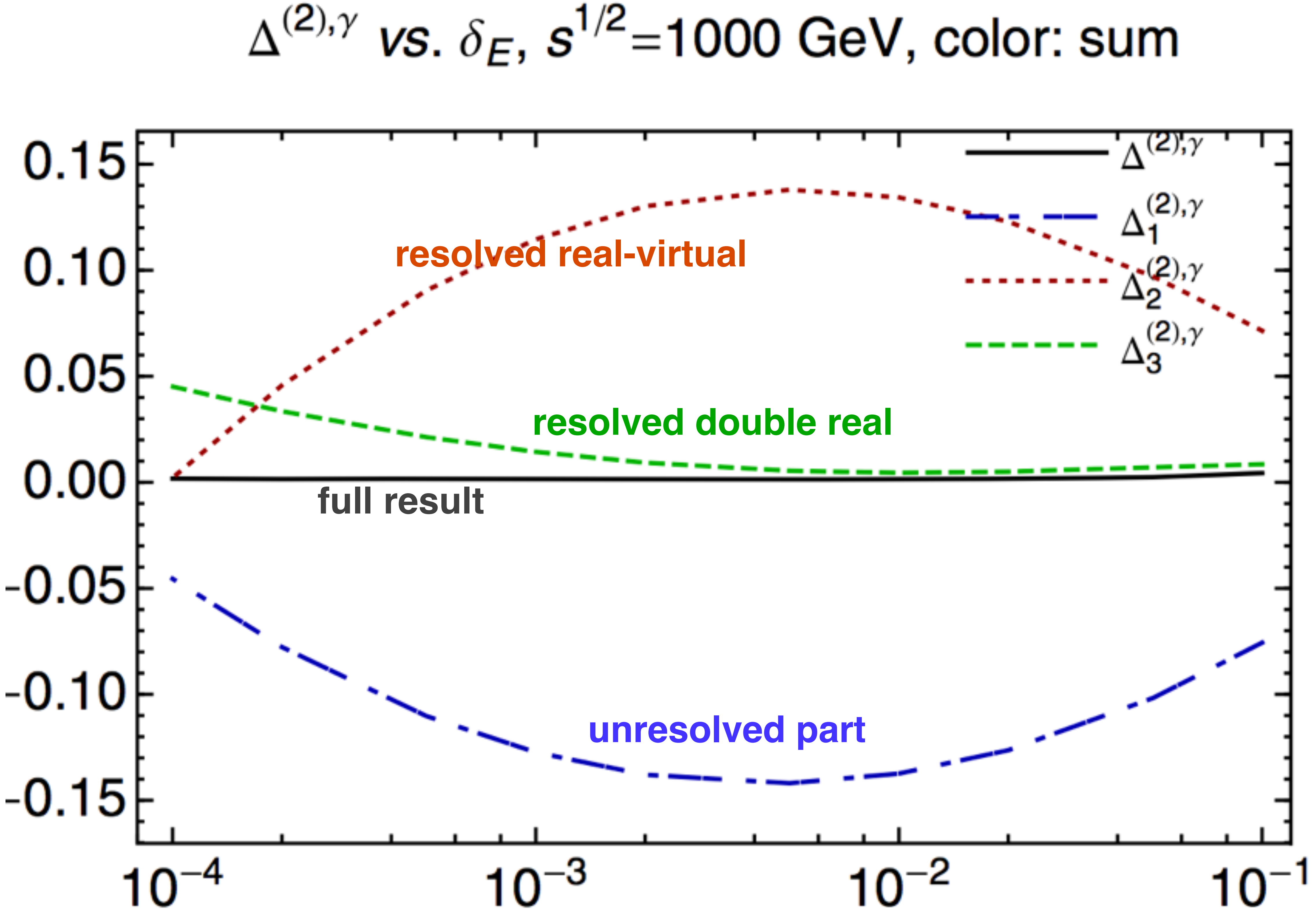

$$\sigma_{\mathrm{NNLO},\gamma} = \sigma_{\mathrm{LO},\gamma}(1 + \Delta^{(1),\gamma} + \Delta^{(2),\gamma})$$

Inclusive Xsec: compare with threshold and high energy expansion

$$\sigma_{\mathrm{NNLO},\gamma} = \sigma_{\mathrm{LO},\gamma}(1 + \Delta^{(1),\gamma} + \Delta^{(2),\gamma})$$

J. Gao, H.X.Z, PRD90.114022; see also Dekkers, Bernreuther, PLB738(2014)325

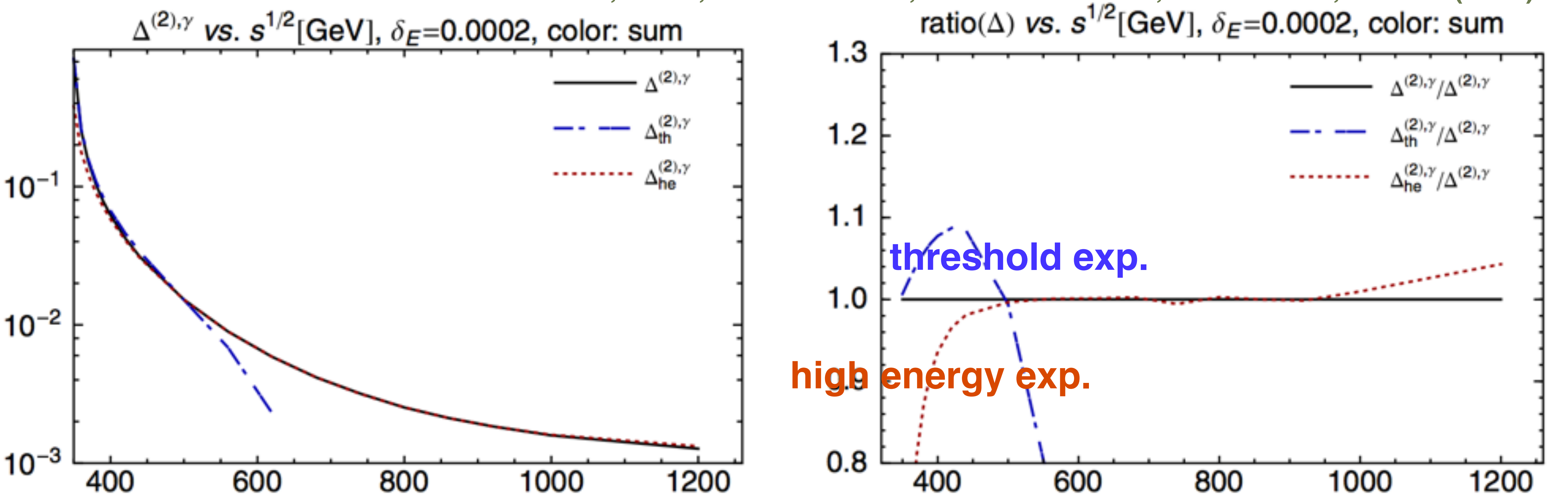

- **Two-loop threshold expansion: [Czarnecki, Melnikov, 1998; Beneke, Signer, Smirnov, 1998; Hoang, Teubner, 1998…]**
- **Two-loop high energy expansion: [Chetyrkin, Harlander, Kuhn, Steinhauser, 1997]**
- **Small corrections, every contribution matter!**
- **Fully closed fermion loop contribution very helpful in checking our calculation [Hoang, Teubner, NPB519 (1998) 285]**

Comparison with Pade approximation

J. Gao, H.X.Z, PRD90.114022

$$\sigma_{\mathrm{NNLO},\gamma} = \sigma_{\mu^+\mu^-,\gamma}\left(R^{(0)} + \frac{\alpha_s(\mu^2)}{\pi} C_F R^{(1)} + \left(\frac{\alpha_s(\mu^2)}{\pi}\right)^2 R^{(2)}\right)$$

$$r = 2m_t/\sqrt{S}$$

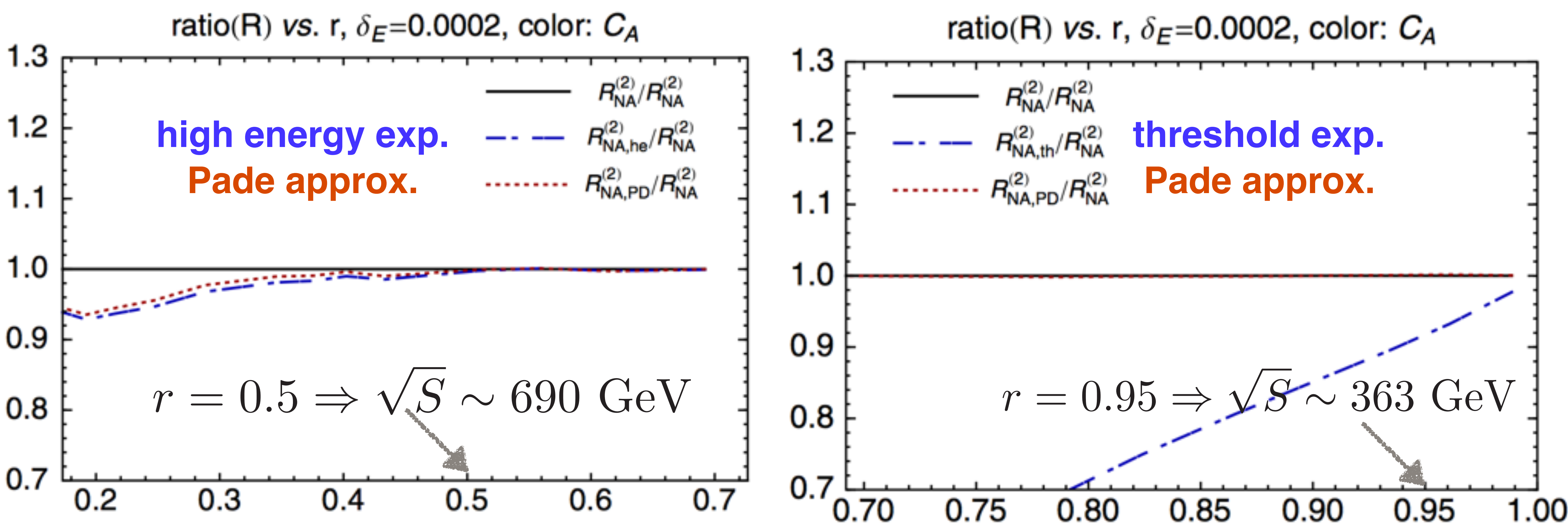

- Two-loop Pade approximation: [Chetyrkin, J. H. Kuhn, and M. Steinhauser, NPB482, 213(1996)]. Three-loop also available [Kiyo et al., NPB823(2009)269]
- In general good agreement exact at very high energy S>(1000GeV)^2. Large power corrections proportional to δ_E*logδ_E*log^2(S/m_t^2) in the numerical calculation

NNLO reduces scale uncertainties

J. Gao, H.X.Z, PRD90.114022

$$\sigma_{\mathrm{NNLO},\gamma} = \sigma_{\mathrm{LO},\gamma}(1 + \Delta^{(1),\gamma} + \Delta^{(2),\gamma})$$

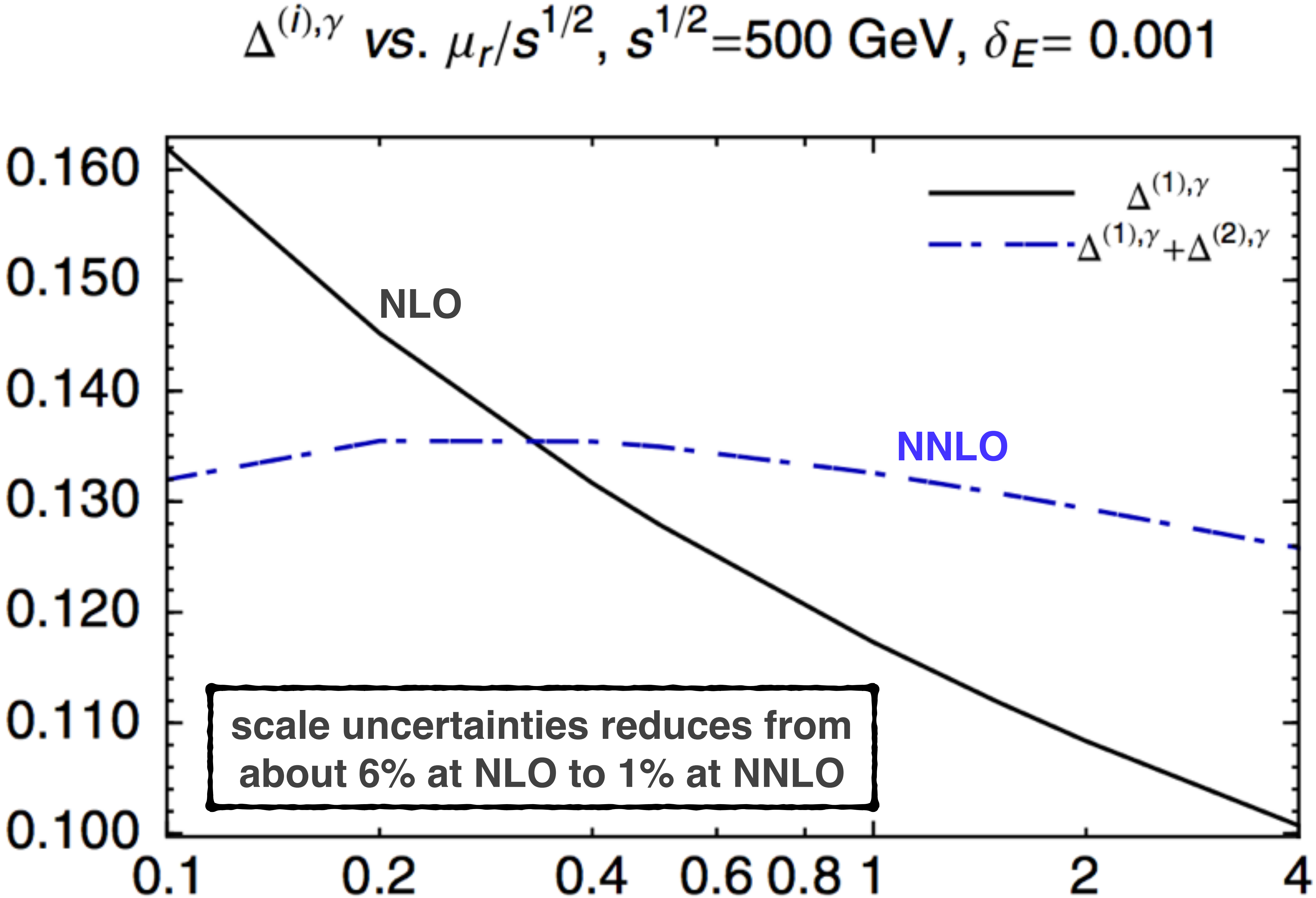

Differential distribution at NNLO

$$\sigma_{NNLO} = \sigma_{LO}\left(1 + \Delta^{(1)} + \Delta^{(2)}\right)$$

J. Gao, H.X.Z, PRL113(2014)262001

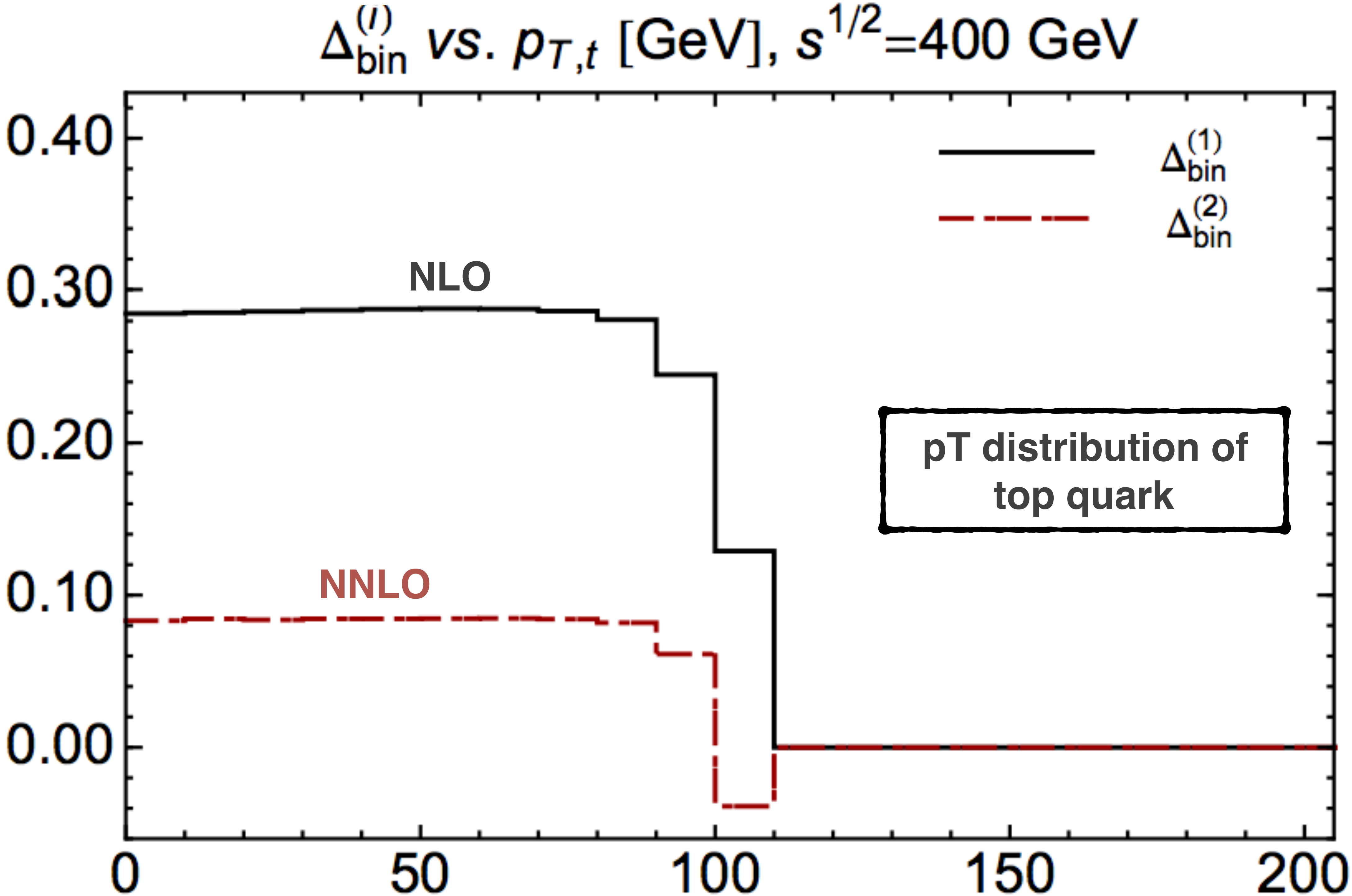

NNLO corrections to forward-backward asymmetry

J. Gao, H.X.Z, PRL113(2014)262001

$$A_{FB} = \frac{\sigma_A}{\sigma_S} \equiv \frac{\sigma(\cos\theta_t > 0) - \sigma(\cos\theta_t < 0)}{\sigma(\cos\theta_t > 0) + \sigma(\cos\theta_t < 0)}$$

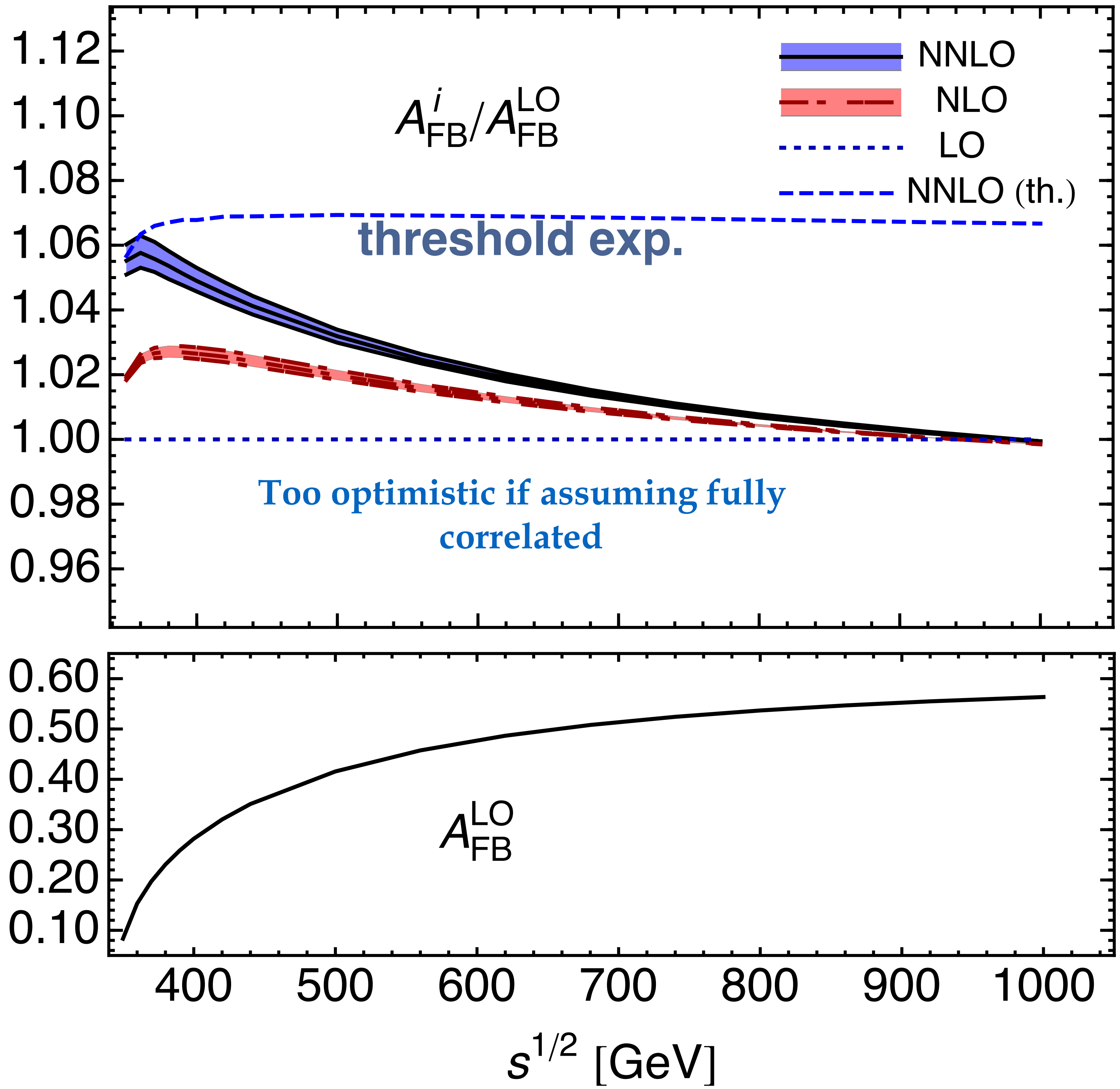

- Estimation of the theoretical uncertainties from scale variations requires assumption on correlations of the Forward and Backward bins
- Fully correlated scale setting leads to too small uncertainties

NNLO corrections to forward-backward asymmetry

J. Gao, H.X.Z, PRL113(2014)262001

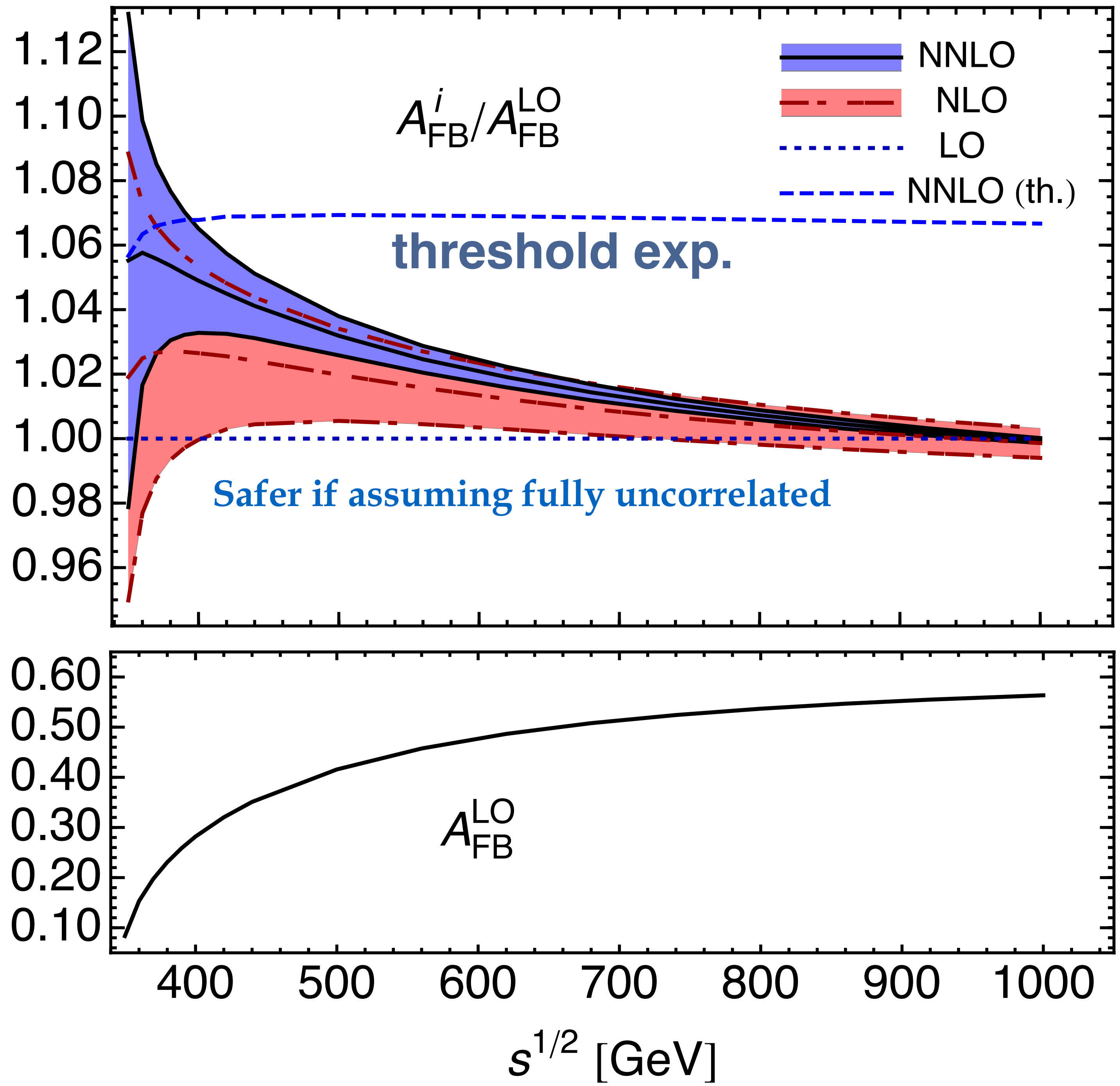

- Uncorrelated scale setting leads to more realistic uncertainties estimate
- Large NNLO QCD corrections even at √S=500GeV (about half the size of NLO corrections)
- NLO EW corrections about 10% [Fleischer et al., EPJC31 (2003) 37]
- NNLO EW corrections highly desirable

Forward-Backward asymmetry bin-by-bin

J. Gao, HXZ, PRL113(2014)262001

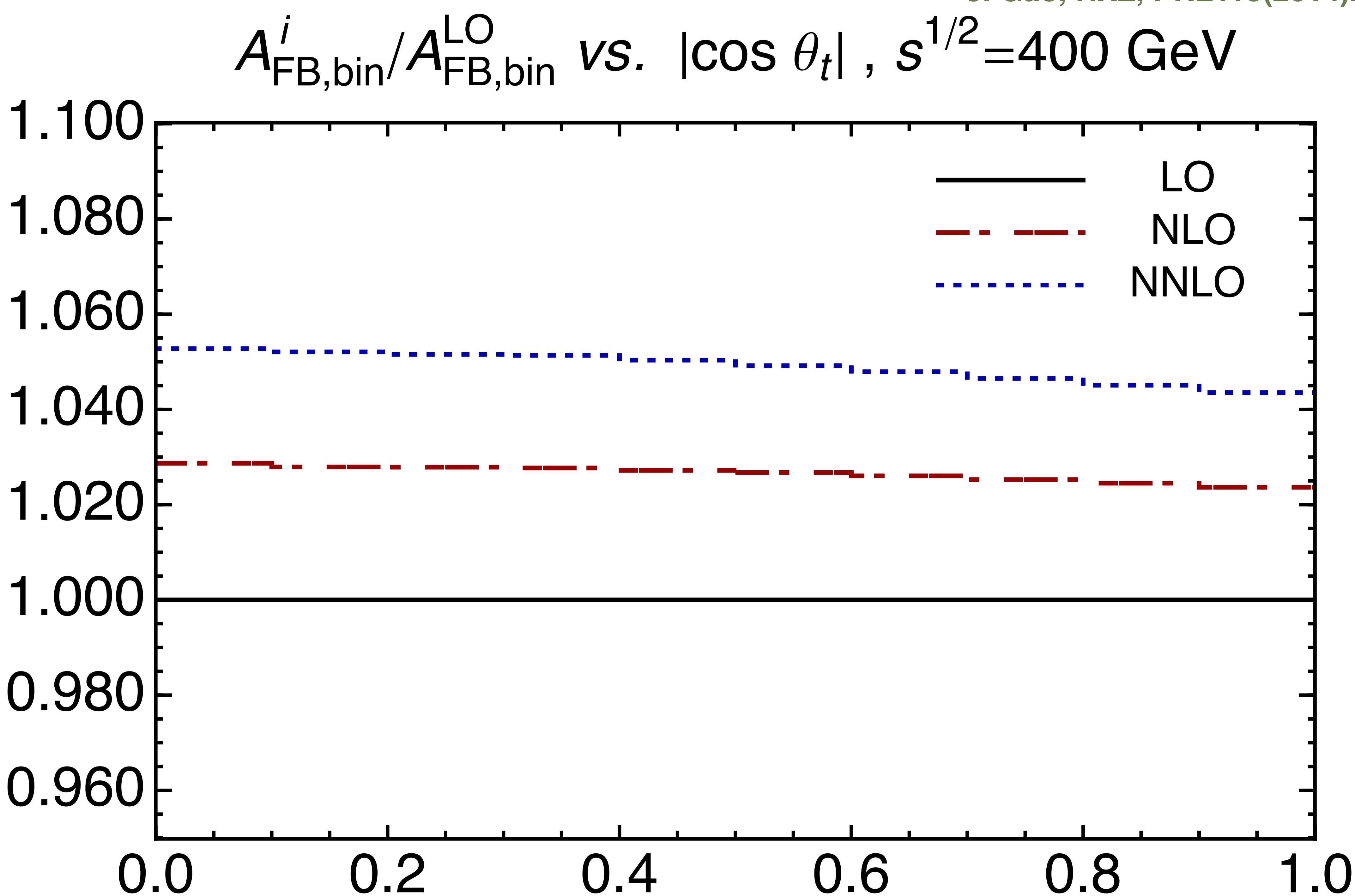

- Our results provide full kinematic dependence allowing for corrections of experimental acceptance

Going beyond stable top production

- Now NNLO QCD corrections to tT production at LC, and NNLO QCD corrections to top decay are available
- It would be interesting to combine production and decay at NNLO to allow full spin correlation and parton level fiducial cross section
- Example: first t-channel single top production and decay at NNLO

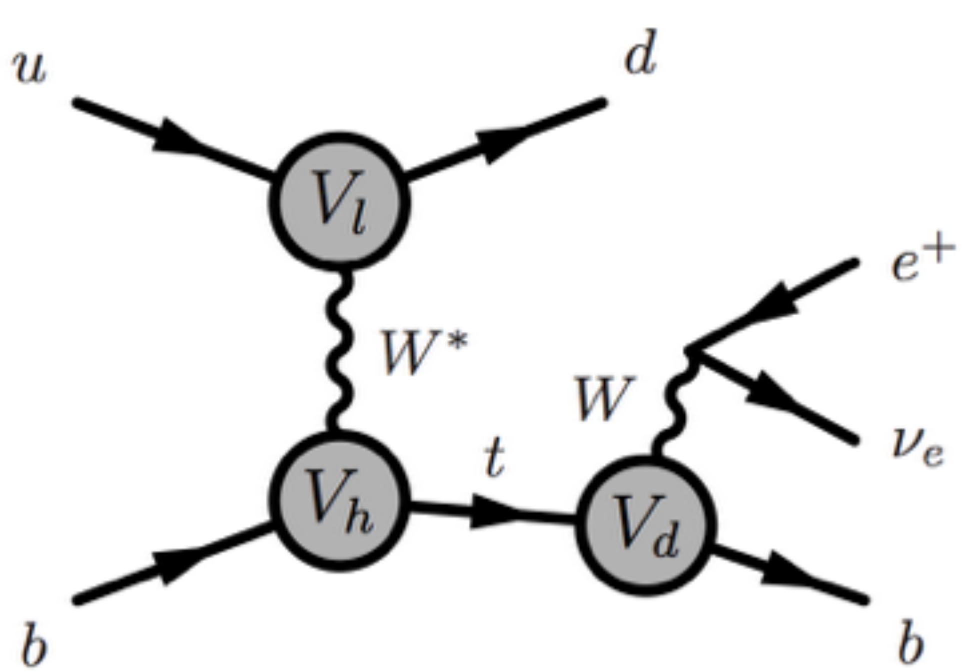

Structure function approximation

Berger, Gao, Yuan, HXZ, 1606.08463

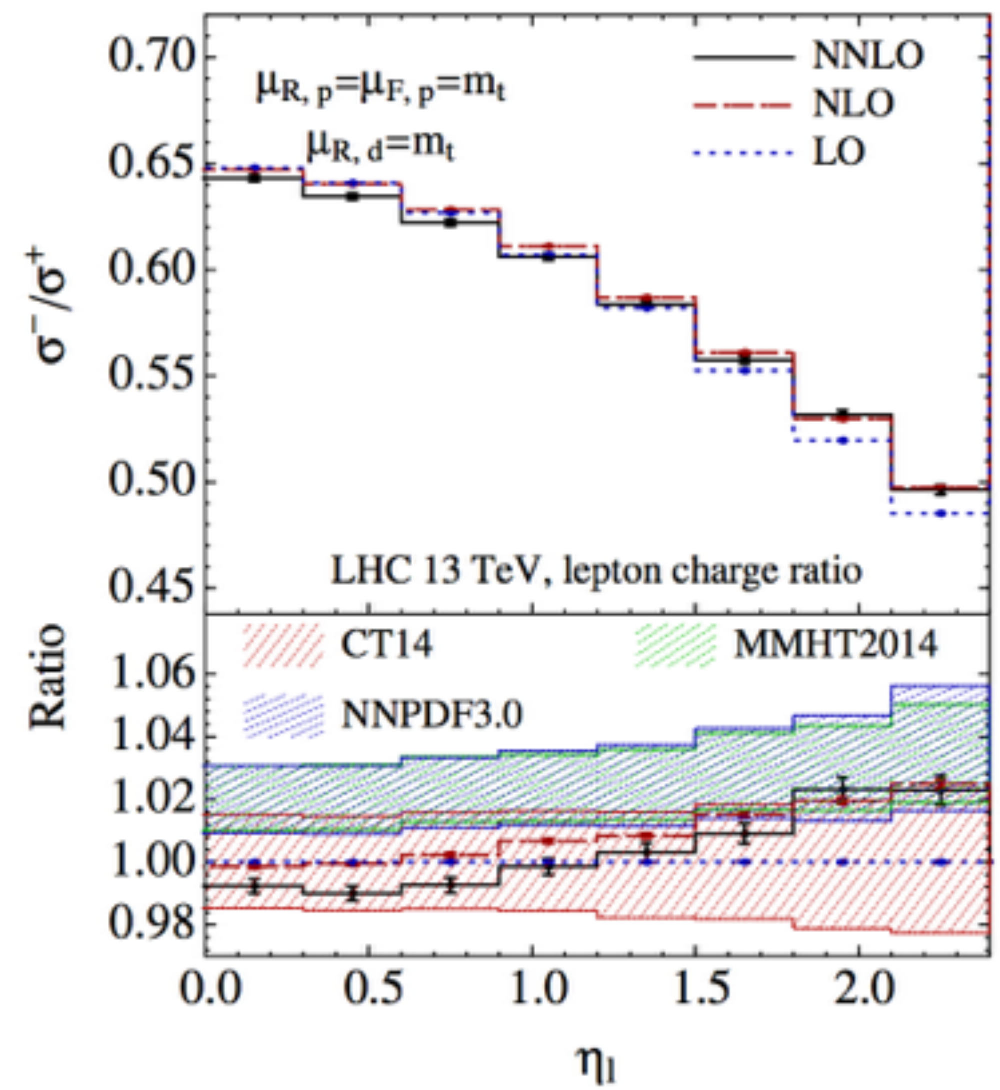

Summary

- Precision calculation for top pair production at LC has long been a theoretical arena.
- Full NNLO QCD corrections for tT production in the continuum now available after many years of effort of different groups
- Large NNLO corrections to FB asymmetry (half the size of NLO corrections). Uncertainties reduce to 0.5% in absolute size at $\sqrt{S}$=500GeV with conservative estimate
- With the current accuracy of QCD prediction, two-loop EW corrections become highly important and might become the driving force of further theoretical progress in the years to come

Thanks a lot for listening!

Backup slide

$$\sigma_{NNLO} = \sigma_{LO}\left(1 + \Delta^{(1)} + \Delta^{(2)}\right)$$

J. Gao, H.X.Z, PRL113(2014)262001